

Finite Element Analysis of Single-Phase Induction Motors

Dániel Marcsa, Miklós Kuczmann
 Széchenyi István University,
 Győr, Egyetem tér 1, Hungary, H-9026, email: marcsadaniel@yahoo.co.uk

Abstract: The single-phase induction motor of the Problem No. 30a of TEAM Workshops has been solved by the Finite Element Method (FEM) using the $A, V - A$ - potential formulation and the $T, \Phi - \Phi$ - potential formulation. This linear problem has been solved in the frequency domain by the two potential formulations.

Keywords: Finite element method, induction motor, eddy current field potential formulation, velocity effects, power dissipation.

1. Introduction

This paper presents the solution of the single-phase induction motor of the Problem No. 30a of TEAM Workshops [1] by using different potential formulations and the Finite Element Method (FEM) [2,3,4]. The linear problem has been solved in the frequency domain by the two potential formulations, and the solutions of them have been compared. Here, the problem is a linear eddy current field problem.

The used potential formulations of motional two dimensional time-stepping Finite Element Method [4,5,6,7] by means of the $A, V - A$ - potential formulation with motion [6,7] and by the $T, \Phi - \Phi$ - potential formulation with motion [8,9] have been implemented. The two-dimensional linear time varying eddy current field problem has been solved in the frequency domain [10] by the two potential formulations.

The used methods are applied to compute the power dissipation of rotor, and rotor steel [11,12] of this single-phase motor. These quantities are computed on a per unit depths (1m) basis.

The induction motor under investigation is considered to be an eddy current field problem. The eddy current field of the motor is assumed to be two dimensional, i.e. the influence of the end-region fields have has been neglected.

2. Arrangement of Induction Motor

The arrangement of the problem is shown in Fig. 1, which is a single-phase induction motor. In Fig.1. σ is the conductivity, μ_r is the relative permeability in the problem. In this figure

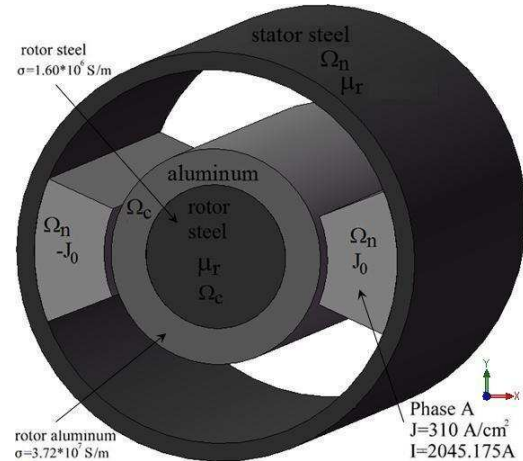


Figure 1. The 3D model of the simulated single-phase induction motor.

the current excitation of the windings is represented by the source current density J_0 . In the $A, V - A$ - potential formulation the inverse model of constitutive relations, or the variable $v_r = 1/\mu_r$ In the $T, \Phi - \Phi$ - potential formulation the direct model of constitutive relations is used.

The rotor is made of rotor steel and rotor aluminum, i.e. the rotor steel is surrounded by the rotor aluminum. The stator steel is laminated and its conductivity has been selected as $\sigma = 0$. The windings are not embedded in slots. The rotation of the rotor is counterclockwise. The range of computation of the single-phase induction motor for rotor angular velocities is from 0 to 358 rad/s (0.95% of the peak field speed) The synchronous speed is $\Omega = 2\pi f = 377 \text{ rad/s}$, because the winding is excited at $f = 60 \text{ Hz}$.

The studied eddy current field problem is separated into two parts. The conductor region, i.e. the rotor, Ω_r and the nonmagnetic, and non-conductive region, the windings, the air, and the laminated stator steel, Ω_n . The Maxwell's equations in the eddy current free region, model a static magnetic field, while in the eddy current region, the "quasi-static" Maxwell's equations are valid. The boundary Γ_B is the closing boundary of the problem region, where normal component of magnetic flux density is neglected.

2. Numerical Simulation Procedures

First of all, from the Physics menu, select the Model Settings, and from the Equation System Form list select the Weak form.

The constants (e.g. moving velocity ω_v , frequency f , external current density \mathbf{J}_0) must be typed in the Options/Constants menu.

2.1. Modeling Motion

In induction machines consider a rotor moving in one direction with velocity \mathbf{v} relative to a reference frame $\mathbf{O}(x,y)$ and a local reference frame $\mathbf{O}'(x',y')$, which is moving with the rotor [7].

The displacement currents are negligible, because of the low frequencies used in the electrical machines, and the Maxwell's equations can be written in the fixed reference frame as:

$$\nabla \times \mathbf{H} = \mathbf{J}, \quad (1)$$

$$\nabla \times \mathbf{E} = -j\omega \mathbf{B}, \quad (2)$$

$$\nabla \cdot \mathbf{B} = 0, \quad (3)$$

$$\mathbf{J} = \begin{cases} \mathbf{J}_0 & \text{in } \Omega_n, \\ \sigma \mathbf{E} & \text{in } \Omega_c. \end{cases} \quad (4)$$

Electromagnetic phenomena are described by the same Maxwell's equations in the fixed, and in the moving reference frames.

$$\begin{aligned} \mathbf{B}' &= \mathbf{B}, \\ \mathbf{E}' &= \mathbf{E} + \mathbf{v} \times \mathbf{B}, \\ \mathbf{H}' &= \mathbf{H}, \\ \mathbf{J}' &= \mathbf{J}, \end{aligned} \quad (5)$$

where the quantities observed from the moving reference frame \mathbf{O}' are marked by apostrophes.

Only the electric field intensity vector \mathbf{E} is modified, because of adding the motion voltage term $\mathbf{v} \times \mathbf{B}$ to \mathbf{E} .

Substituting the equation of \mathbf{E}' into (4) gives the next relation:

$$\mathbf{J} = \sigma \mathbf{E}' = \sigma (\mathbf{E} + \mathbf{v} \times \mathbf{B}), \quad (6)$$

because the motion of the conductor region of the induced induction motor eddy currents, and the eddy currents are depending on the velocity.

The velocity \mathbf{v} has been type in the Options/Expressions/ Subdomain Expressions the following form $\mathbf{v} = \omega_v \times \mathbf{r}$ by separate the x, y -components.

2.2. The $A, V - A$ - potential formulation with motion

This potential formulation coupled with moving velocity seems to be the most widely used formulation of electrical machines [4,5,6].

The $A, V - A$ - potential formulation is based on the magnetic vector potential \mathbf{A} and the electric scalar potential V with nodal element approximation.

Basically, the induction motor is a two-dimensional problem, and this results in the two dimensional case that the electric scalar potential can be selected as $V=0$ in the $A, V - A$ - potential formulation [2].

The divergence-free magnetic flux density \mathbf{B} can be described by the curl of the magnetic vector potential \mathbf{A} , i.e.

$$\mathbf{B} = \nabla \times \mathbf{A}. \quad (7)$$

The curl of magnetic vector potential \mathbf{A} weak form is the following: $Azy - Azx$, where Azy is x -component of magnetic flux density \mathbf{B} , and $-Azx$ is the y -component.

Substituting the equation (7) into Faraday's law (2) gives the next equation:

$$\nabla \times \mathbf{E} = -j\omega \nabla \times \mathbf{A}, \quad (8)$$

since $V=0$.

Redistribute and substitute the $\mathbf{E}' = \mathbf{E} + \mathbf{v} \times \mathbf{B}$ into the equation (8), and the use of relation (7) result in the $A, V - A$ - potential formulation with motion in the conductive region Ω_c in the frequency domain,

$$\nabla \times (\nu \nabla \times \mathbf{A}) + \sigma (j\omega \mathbf{A} - \mathbf{v} \times \nabla \times \mathbf{A}) = \mathbf{0}, \quad (9)$$

where reluctivity $\nu = 1/(\mu_0 \mu_r)$.

The (9) equation is typed in the Physics/Equations System/ Subdomain Settings the following form:

$$\begin{aligned} & (1/\mu) * ((Azy * Azy_test) + (Azx * Azx_ \\ & test)) + \sigma * \\ & ((test(Az) * (j * \omega * Az)) - test(Az) * (- \\ & Vx * Azx - Vy * Azy)), \end{aligned}$$

where Azy_test , and $test(Az)$ are the test functions.

In the non-conducting region, Ω_n , the fundamental equation is given by

$$\nabla \times (\nu \nabla \times \mathbf{A}) = \mathbf{J}_0, \quad (10)$$

where ν_0 is the reluctivity in vacuum.

At the $A, V - A$ - potential formulation the motion voltage term weak form is the following: $(-Vx * Azx - Vy * Azy)$.

2.3. The $T, \Phi - \Phi$ - potential formulation with motion

Basically this potential formulation has not been used in the simulation of induction machines, but some papers in the literature can be found from the other part of FEM analysis [8,9].

The $T, \Phi - \Phi$ - potential formulation is based on the current vector potential T with edge element approximation and on the reduced magnetic scalar potential Φ with nodal element approximation.

The source current density J_0 can be written by the curl of the impressed current vector potential T_0 [2,3],

$$J_0 = \nabla \times T_0. \quad (11)$$

The above equation has been written in weak form:

$$((T_0 y_x - T_0 x y - J_z) * (T_0 y_x_test - T_0 x y_test)).$$

The expression of the magnetic field intensity H and the eddy current density J are then from (2) are:

$$H = T_0 + T - \nabla \Phi, \quad (12)$$

$$J = \nabla \times T, \quad (13)$$

because $\nabla \cdot J = 0$.

In this formulation, the electric field intensity E with motion voltage term is the following:

$$E' = \frac{1}{\sigma} \nabla \times T + v \times B. \quad (14)$$

Combining the Faraday's law (2), the constitutive relation $B = \mu H$, the equation (12), and the equation (14) results in the following partial differential equation:

$$\nabla \times \left(\frac{1}{\sigma} \nabla \times T + v \times (T_0 + T - \nabla \Phi) \right) = -j\omega \mu T_0 - j\omega \mu T + j\omega \mu \nabla \Phi, \quad (15)$$

where $\mu = \mu_0 \mu_r$ is the permeability.

The weak formulation of (15) equation is the following:

$$\begin{aligned} & (T y_x_test - T x y_test) * \\ & (1/\sigma * (T y_x - T x y) + \\ & (V x * \mu * (T_0 y + T y - F I y) - \\ & V y * \mu * (T_0 x + T x - \\ & F I x))) + j * \omega * \mu * (T x_test * (T_0 x + T x - \\ & F I x) + T y_test * (T_0 y + T y - F I y)), \end{aligned}$$

where $1/\sigma * (T y_x - T x y)$ is the electric field intensity E .

Substituting the equation (12) into the magnetic Gauss' law (3) gives the next partial differential equation:

$$\nabla \cdot \mu (T_0 + T - \nabla \Phi) = 0. \quad (16)$$

The weak form of this equation:

$$\begin{aligned} & j * \omega * \mu_0 * \mu_r * (F I x * test(F I x) + F I y * test(F I y)) - \\ & j * \omega * \mu_0 * \mu_r * (T_0 x * test(F I x) + T_0 y * test(F I y)) - \\ & j * \omega * \mu_0 * \mu_r * (T x * test(F I x) + T y * test(F I y)). \end{aligned}$$

In the non-conducting region, Ω_n , only equation (16) has to be solved, but $\mu = \mu_0$, and $T = 0$.

At this formulation the motion voltage term weak form is the following:

$$\begin{aligned} & (V x * \mu * (T_0 y + T y - F I y) - \\ & V y * \mu * (T_0 x + T x - F I x)). \end{aligned}$$

2.4. The Power Dissipation

The average power dissipation due to eddy current losses can be found by the power density loss can be integrated over the surface,

$$P_d = \int_{\Omega} \Re \left(\frac{1}{2} \sigma E \cdot E^* \right) d\Omega, \quad (17)$$

where the real part of power density loss $\frac{1}{2} \sigma E \cdot E^*$ can be integrated over the surface of the body Ω , and E is the electric field intensity, and E^* conjugacy of electric field intensity.

The computation of power dissipation the (17) equation weak form type the Postprocessing/Subdomain Integration menu.

At the $A, V - A$ - potential formulation the weak form is the next:

$$0.5 * \text{real}((\sigma * ((-j * \omega * A_z) + (-V_x * A_{zx} - V_y * A_{zy}))) * (\text{conj}((-j * \omega * A_z) + (-V_x * A_{zx} - V_y * A_{zy}))))),$$

and the other potential formulation:

$$0.5 * \text{real}(\sigma * (1/\sigma * (T y_x - T x y))) * (\text{conj}(1/\sigma * (T y_x - T x y)))).$$

The difference between the above two weak form is the moving velocity. This is cause, at the $T, \Phi - \Phi$ - formulation after the simulation the $E' = E$, whereas the $A, V - A$ - potential after the simulation the $E' = E + v \times B$ remain.

3. Expected Results

The numerical computations were performed using computer programs developed by the functions of COMSOL Multiphysics. The programs have been run on an Intel(R) Core(TM)2 Duo CPU T9300 with the clock frequency of the processor 2.50 GHz with 2Gbyte RAM.

All the linear simulations have been studied using the same mesh, which consists of 21208 second-order triangular elements as it can be seen on the Fig. 2a. The Fig. 2b shows the used mesh to calculate the impressed current vector potential and the closing boundary consists of 55936 second-order triangular elements. The number of unknowns are different in the two potential formulations. Using the $A, V - A$ - formulation, the number of unknowns is 42733, and in case of the $T, \Phi - \Phi$ - formulation the number of unknowns is 63517.

The CPU time for the analysis at high speeds is more that at standstill. The CPU time is increased when the speed becomes high, because the number of iteration for the GMRES solver (Generalized Minimum Residual Method) with SSOR preconditioner (Symmetric Successive Over-Relaxation) method is increased due to the ill-condition of the mass matrix [13]. Generally,

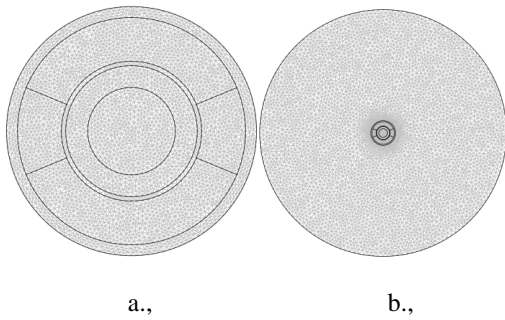


Figure 2. Finite element meshes of the studied motor.

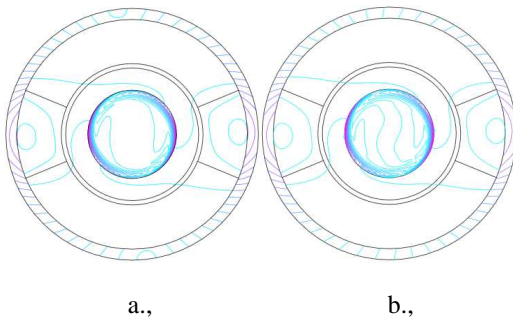


Figure 3. The magnetic flux density lines at 358 rad/s angular velocity.

computation programs take into account the symmetry of the global matrix, and storing only the half of this matrix in memory. However, in this case the whole matrix must be stored [5].

The computed absolute value of magnetic flux density lines inside the simulated motor for the running at 358 rad/s can be seen in Fig. 3. The solution of $A, V - A$ - formulation is shown in Fig. 3a, and the other potential formulations solution is shown in Fig. 3b. These two solutions seem to be equal aside from the little difference inside the rotor steel. The solutions is seem to be equal in all simulations.

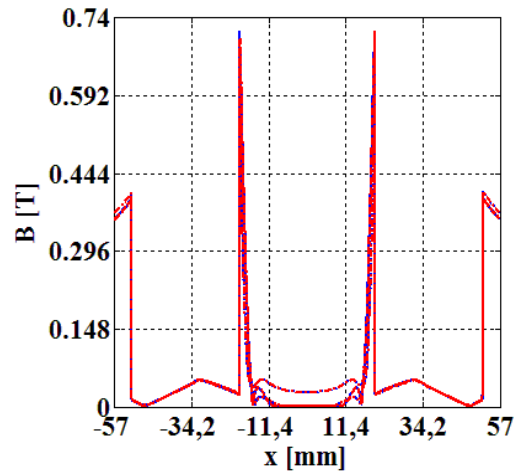


Figure 4. Computed magnetic flux inside the simulated motor across the x -axis.

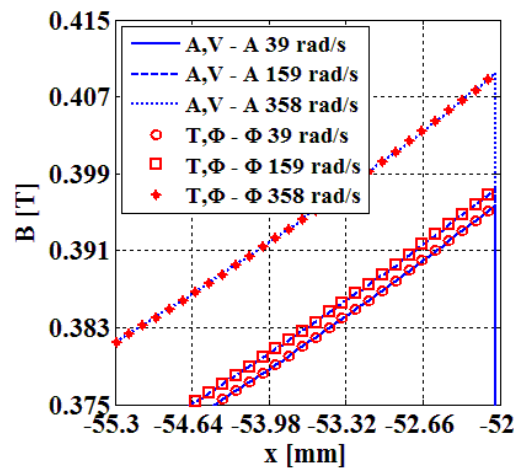


Figure 5. Magnetic flux difference between the potential formulations.

The absolute value of magnetic flux density along the line inside the simulated induction motor $x = -0.057, \dots, 0.057$ mm, $y=0$ can be seen in Fig. 4. This figure shows the results of analysis at 39 rad/s, 159 rad/s, and 358 rad/s angular velocities.

Fig. 5 shows an enlarged region in $x = -0.0553, \dots, -0.052$ mm, e.i. the magnetic flux density inside the stator steel can be seen. The solutions of potential formulations seem to be equal at three different angular velocities. This phenomenon can come true at all angular velocities of simulation.

The rotor loss is computed as a sum of the power dissipation of rotor steel and rotor aluminum. A comparison between the computed rotor loss of two potential formulations as functions of angular velocity is shown in Fig. 6.

A comparison between the computed steel loss of two potential formulations as functions of angular velocity is depicted in Fig. 7. The maximum of relative is less than 1%. This difference results that these potential formulations are depending on the quality of mesh as well. The $A, V - A$ - potential formulation solutions are the minor of the "good" solution, whereas the $T, \Phi - \Phi$ - potential formulation solutions are the major of the "good" solution. The curves of the results can be seen in the Fig. 7.

4. Conclusion

The used numerical procedure of eddy current field calculation results in the expected data. The two different potential formulations in frequency domain solutions have been compared and the results seem to be close to each other.

In the two dimensional case, $A, V - A$ - potential formulation seems to be a better solver with motion voltage term. The $A, V - A$ - potential formulation with motion voltage term converged faster, the number of elements and unknowns are less than the $T, \Phi - \Phi$ - potential formulation with motion voltage term.

The aim of further research is to compute the torque, the induced voltage of windings, and compared with the analytical solution of the Problem No. 30a of TEAM Workshops.

Furthermore, the aim of further research is to solve this problem by the $T, \Phi - \Phi$ - formulation and the $A, V - A$ - formulation taking the nonlinearity into account, and to compare these nonlinear solutions.

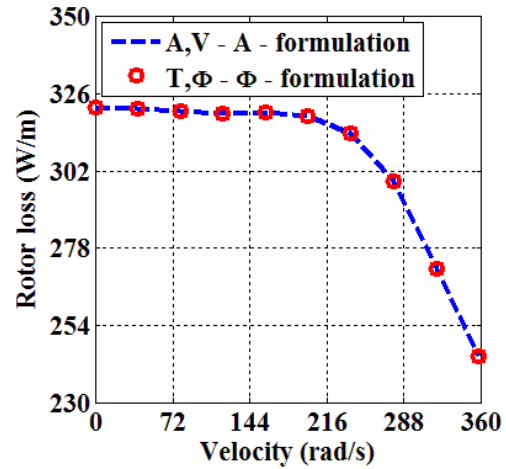


Figure 6. Computed rotor loss as functions of velocities.

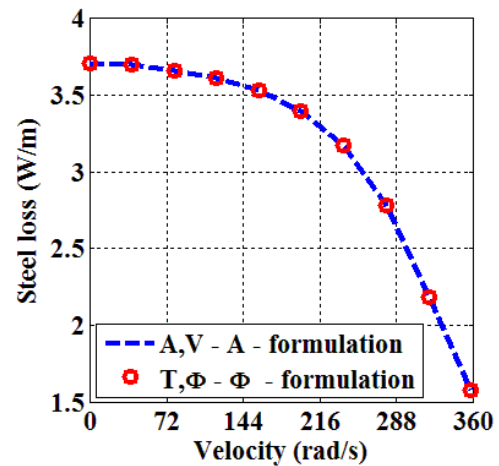


Figure 7. Computed steel loss as functions of velocities.

5. References

- [1] Induction Motor Analysis – International TEAM Benchmark Problem No. 30a, Testing Electromagnetic Analysis Methods (T.E.A.M.), <http://www.compumag.co.uk/>
- [2] M. Kuczmann, A. Iványi, *The Finite Element Method in Magnetics*, Akadémiai Kiadó, Budapest, printed in 2008.
- [3] Bíró O., Richter K. R., CAD in electromagnetism, In *Series Advances in Electronics and Electron Physics*, Academic Press, New York, 1991, pp. 82.

- [4] Antero Arkkio, *Analysis of Induction Motors Based on the Numerical Solution of the Magnetic Field and Circuit Equations*, Electrical Engineering Series, No. 59, Acta Polytechnica Scandinavica, Helsinki University Of Technology, 1987.
- [5] J. P. A. Bastos, N. Sadowski, *Electromagnetic Modeling by Finite Element Methods*, Marcel Dekker Inc., New York - Basel, 2003.
- [6] H. De Gersen, K. Hameyer, Comparison of motional and nonmotional time-harmonic finite element simulation of solid rotor single-phase induction machines, *Journal of Technical Physics*, , vol. 43, no. 4, pp. 389-397,2002.
- [7] N. Burais, A. Foggai, A. Nicolas, J. P. Pascal, J. C. Sabonnadiere, Numerical Solution of Eddy Currents Problems Including Moving Conducting Parts, *IEEE Transaction on Magnetics*, Vol. MAG-20, No. 5, 1984, pp. 1995-1997.
- [8] A. Slama, V. Mazauric, Y. Maréchal, G. Meunier, Electric Railgun 3D modeling: Computation of eddy currents and Lorenz force, *IEEE Transaction on Magnetics*, Vol. 37, No. 1, 2001, pp. 139-142.
- [9] O. Chadebec, G. Meunier, V. G. Mazauric, Y. Le Floch, P. Labie, Eddy-Current Effects in Circuit Breakers During Arc Displacement Phase, *IEEE Transaction on Magnetics*, Vol. 40, No. 2, 2004, pp. 1358-1361.
- [10] Biro O. Edge element formulations of eddy current problems, *Comput. Meth. Appl. Mech. Eng.* Vol. 169, 1999, pp. 391-405.
- [11] K. R. Davey, Rotating field analysis using boundary element methods, *IEEE Transactions on Magnetics*, Vol. 35, No. 3, 1999, pp. 1402-1405.
- [12] Ivanyi A. *Magnetic field computation with R-functions*, Akadémiai Kiadó, Budapest, 1998.
- [13] K. Muramatsu, N. Takahashi, T. Hashio, C. Yamada, M. Ogawa, S. Kobayashi, T. Kuwahara, 3-D Eddy Current Analysis in Moving Conductor of Permanent Magnet Type of Retarder Using Moving Coordinate System, *IEEE Transaction on Magnetics*, Vol. 14, No. 4, 1999, pp. 1312-1317.

6. Acknowledgements

This paper was supported by the János Bolyai Research Scholarship of the Hungarian Academy of Sciences (BO/00064/06), by EPCOS Ltd., by Széchenyi István University (12-3210-02), and by the Hungarian Scientific Research Fund, OTKA PD73242.